Transient and Persistent Dendritic Spines in the Neocortex In Vivo

Anthony J.G.D. Holtmaat,[1] Joshua T. Trachtenberg,[1,3] Linda Wilbrecht,[1] Gordon M. Shepherd,[1] Xiaoqun Zhang,[1] Graham W. Knott,[2] and Karel Svoboda[1,*]
[1]Howard Hughes Medical Institute
Cold Spring Harbor Laboratory
Cold Spring Harbor, New York 11724
[2]Institut de Biologie Cellulaire et de Morphologie
Université de Lausanne
Rue du Bugnon 9
CH 1005 Lausanne
Switzerland

Summary

Dendritic spines were imaged over days to months in the apical tufts of neocortical pyramidal neurons (layers 5 and 2/3) in vivo. A fraction of thin spines appeared and disappeared over a few days, while most thick spines persisted for months. In the somatosensory cortex, from postnatal day (PND) 16 to PND 25 spine retractions exceeded additions, resulting in a net loss of spines. The fraction of persistent spines (lifetime $\geq$ 8 days) grew gradually during development and into adulthood (PND 16–25, 35%; PND 35–80, 54%; PND 80–120, 66%; PND 175–225, 73%), providing evidence that synaptic circuits continue to stabilize even in the adult brain, long after the closure of known critical periods. In 6-month-old mice, spines turn over more slowly in visual compared to somatosensory cortex, possibly reflecting differences in the capacity for experience-dependent plasticity in these brain regions.

Introduction

In the mammalian neocortex, neural circuits are sculpted by spontaneous and sensory-evoked activity (Katz and Shatz, 1996). Although plasticity is most rapid and robust during early postnatal development (Katz and Shatz, 1996), sensory representations in the adult cortex remain dynamic (Darian-Smith and Gilbert, 1994; Daw et al., 1992; Diamond et al., 1994; Fox, 2002; Gilbert, 1998; Wang et al., 1995).

Functional rewiring of cortical circuits may involve structural plasticity with synapse formation and elimination (Antonini and Stryker, 1993; Chklovskii et al., 2004; Knott et al., 2002; Lendvai et al., 2000; Lowel and Singer, 1992; Ramon y Cajal, 1893; Stepanyants et al., 2002; Trachtenberg et al., 2002; Turner and Greenough, 1985; Ziv and Smith, 1996). In particular, recent work has focused on dendritic spines as a possible substrate of circuit plasticity (Bonhoeffer and Yuste, 2002). Spines are tiny dendritic protrusions that receive the vast majority of excitatory synapses (Nimchinsky et al., 2002). Spines emerge to make synapses (Engert and Bonhoeffer, 1999; Maletic-Savatic et al., 1999) or expand (Matsuzaki et al., 2004), in response to synaptic stimulation (Knott et al., 2002; Toni et al., 1999). Long-term in vivo imaging in S1 has revealed that some spines appear and disappear in an experience-dependent manner, associated with synapse formation and elimination, while other spines persist for at least a month (Trachtenberg et al., 2002). In V1, spines were found to be largely persistent (Grutzendler et al., 2002). However, a direct comparison of these studies is complicated because of differences in experimental methods, the age and strain of the mice used, and the cell types involved.

Here, we imaged the apical dendritic tufts of layer (L) 5B and 2/3 neurons in the developing and adult somatosensory and visual cortex to measure the parameters governing dendritic and spine structural plasticity. High-resolution, chronic, time-lapse imaging revealed that a fraction of spines appear and disappear over days, while other spines persist for months. The persistent fraction increased gradually with development and continued to increase in the adult. Spine turnover was more rapid in the somatosensory than in the visual cortex.

Results

In the majority of experiments, we used transgenic mice expressing EGFP in a subset of L2/3, L5, and L6 pyramidal neurons (line GFP-M) (Feng et al., 2000; Trachtenberg et al., 2002). In some experiments, we used a similar transgenic mouse line in which a much larger fraction of the same neuronal subtypes are labeled (line YFP-H) (Feng et al., 2000; Grutzendler et al., 2002). All neurons were reconstructed either from in vivo images or in fixed sections (Experimental Procedures).

To determine whether the GFP-positive cells comprise a normal subset of cortical neurons, we used laser-scanning photostimulation in brain slices to map the spatial distribution of their synaptic input (see the Supplemental Data at http://www.neuron.org/cgi/content/full/45/2/279/DC1/) (Callaway and Katz, 1993; Shepherd et al., 2003). GFP-positive L5B cells and GFP-negative neighbors received indistinguishable patterns of synaptic input (Supplemental Figure S1). We conclude that GFP-positive neurons constitute a functional and representative subset of cortical cells.

Animals were prepared for imaging by implanting a small glass window centered over somatosensory or visual cortex (Experimental Procedures). We used 2-photon laser-scanning microscopy (2PLSM) (Denk et al., 1990; Denk and Svoboda, 1997) to repeatedly image dendrites and their spines during development and in the adult brain.

Pruning of Dendritic Spines during Development

Previous studies in young adult (2 months old) neocortex found that a fraction of dendritic spines appear and disappear over days, while a subpopulation (50%–60%) of spines persists for at least a month of time-lapse

*Correspondence: svoboda@cshl.edu
[3]Present address: Department of Neurobiology, Box 951761, 695 Charles Young Drive South, Los Angeles, California 90095.

imaging (Trachtenberg et al., 2002). How does spine stability change with developmental age? To begin to address this question, we performed chronic imaging experiments in developing S1 spanning the third and fourth postnatal week. These experiments are complicated by the developmental regulation of expression of fluorescent proteins under control of the Thy-1 promoter in the transgenic mice (Feng et al., 2000) (Figures 1A and 1B). Expression in sensory neocortex starts toward the end of the second postnatal week, but at this time only the YFP-H line had adequate numbers of brightly labeled cells for in vivo imaging (Figures 1A and 1B). At postnatal day (PND) 16, a sparse subset of L5B pyramidal cells were labeled in S1 (Figure 1B). Over the time course of the experiment, the field of view became crowded with dendrites and axons that began to express YFP at later time points (Figures 1A and 1B). We focused our analysis on dendritic segments that were separated from neighboring branches and could be tracked over all experimental days.

To monitor spine turnover and stability, we collected high-resolution image stacks of several (five to ten) regions of interest per dendritic tuft (Figure 1C). Around 2 weeks of age, dendritic branches were studded with numerous spines (0.49 $\pm$ 0.13 μm^{-1}; n = 5; PND 16) comprising all commonly described classes, including mushroom-type, stubby, and thin spines (Peters and Kaiserman-Abramof, 1970), as well as long filopodia-like protrusions (Dailey and Smith, 1996; Lendvai et al., 2000; Portera-Cailliau et al., 2003).

The development of dendritic spines was analyzed in daily time-lapse images (922 spines; n = 5) (Figures 1C–1F). Spine densities were higher at younger ages (Figure 1C), implying a net loss of dendritic spines with developmental age. The decrease in spine density did not proceed simply by retraction of dendritic spines; rather, at young ages (PND 16) more than 30% of the spines disappeared, while 25% appeared, between imaging sessions from one day to the next (Figures 1C and 1D). This resulted in a gradual decrease in the spine density (to 0.30 $\pm$ 0.08 μm^{-1} at PND 26) (Figure 1E). A similar decrease in spine density was observed in measurements from naive perfusion-fixed tissue derived from YFP-H mice (0.44 $\pm$ 0.10 μm^{-1}, PND 16–18, n = 10; 0.32 $\pm$ 0.02 μm^{-1}, PND 25–33, n = 3; indistinguishable from the decrease seen in vivo; analysis of covariance). This implies that the developmental decrease in spine density was not due to chronic imaging or developmental changes in detection efficiency of small spines. Rates of spine retraction and addition in vivo decreased with developmental age at different rates, so that at 4 weeks of age addition and subtraction were balanced (Figure 1D). Thereafter, spine densities were relatively stable (Trachtenberg et al., 2002).

We tracked the fates of individual spines observed in the first image and calculated the fraction of spines surviving (survival fraction) as a function of time (Figure 1E). The fraction of spines that persisted for at least 8 days was 35.0% $\pm$ 9.9% (n = 5), much less than that previously observed in young adult mice (Trachtenberg et al., 2002) (53.9% $\pm$ 8.5%; n = 6; $p < 0.05$). This indicates that spine plasticity and stability is regulated during development, after the closure of critical periods in S1 (>PND 15) (Fox, 1992; Stern et al., 2001).

Age-Dependent Regulation of Spine Plasticity and Stability in the Adult Brain

Could spine plasticity be regulated by age even in the adult brain? To answer this question, we imaged the apical dendritic arbors of individual L5B neurons in the S1 cortex of mature adult (age 6 months) GFP-M mice (Figure 2A) and compared the results to our experiments in developing mice (Figure 1) and to previous experiments in young adult mice (Trachtenberg et al., 2002). In the mature adult animals, a subpopulation of spines appeared and disappeared from day to day (n = 5; 1286 spines) (Figure 2B; Supplemental Figures S2A and S2B at http://www.neuron.org/cgi/content/full/45/2/279/DC1/). These spines were usually thin, as judged by their low fluorescence level, compared to bright mushroom spines on the same dendrites, which tended to persist (Figure 2B). Spine densities and daily turnover ratios (TOR, the fraction of spines appearing and disappearing from day to day) were constant over time (density, 0.29 $\pm$ 0.08 μm^{-1}; TOR, 15.4% $\pm$ 1.6%; Figures 2C and 2D) (Trachtenberg et al., 2002). Also in experiments that lasted for several months, spines were seen to appear and disappear during the entire imaging period (Figure 2F; Supplemental Figure S2C). These observations argue against the possibility that spine addition and subtraction were caused by implanting the imaging window.

To compare spine dynamics and stability between different ages and different cortical regions, we calculated the spine survival fraction for each cell as a function of time (survival function [*SF*]). *SF*s could be fit with an exponential function and a constant term. The time constant, τ, of the exponential (a few days) is a measure of the rate of spine turnover. The constant term reflects the persistent fraction (Figure 6A; see Experimental Procedures).

For 6-month-old mice, the *SF* revealed that spines that ultimately disappeared lasted at most a few days after they were formed (τ = 1.9 days; Figures 2E and 6A). We defined spines that persisted for four days or less as "transient" spines. Spines that persisted for 8 days or more are "persistent" spines. Although addition and subtraction of persistent spines was observed (Figure 2G), these events were rare; spines that survived for more than 8 days were highly likely (93%) to persist for the rest of the imaging session, more than 3 weeks (Figure 6A). We further imaged two mice for over 3 months with longer sampling intervals. These experiments confirmed that spines that persisted for 8 days were highly likely to persist for 3 months (Figure 2F). Under conditions of constant sensory experience, transient and persistent spines therefore constitute largely distinct populations.

In 6-month-old mice, the fraction of transient spines was significantly lower (21.4% $\pm$ 4.3% versus 30.2% $\pm$ 6.9%; $p < 0.05$)—and the fraction of persistent spines was significantly larger (72.5% $\pm$ 2.6% versus 53.9% $\pm$ 8.5%; $p < 0.01$)—compared to young adult (5–11 weeks) animals. We noticed that dendrites with low spine densities tend to have higher proportions of transient spines than dendrites with high spine densities (Figure 6C). Therefore, we quantified the density of transient spines per cell as a measure of spine dynamics, which is independent of total spine density and has lower variance.

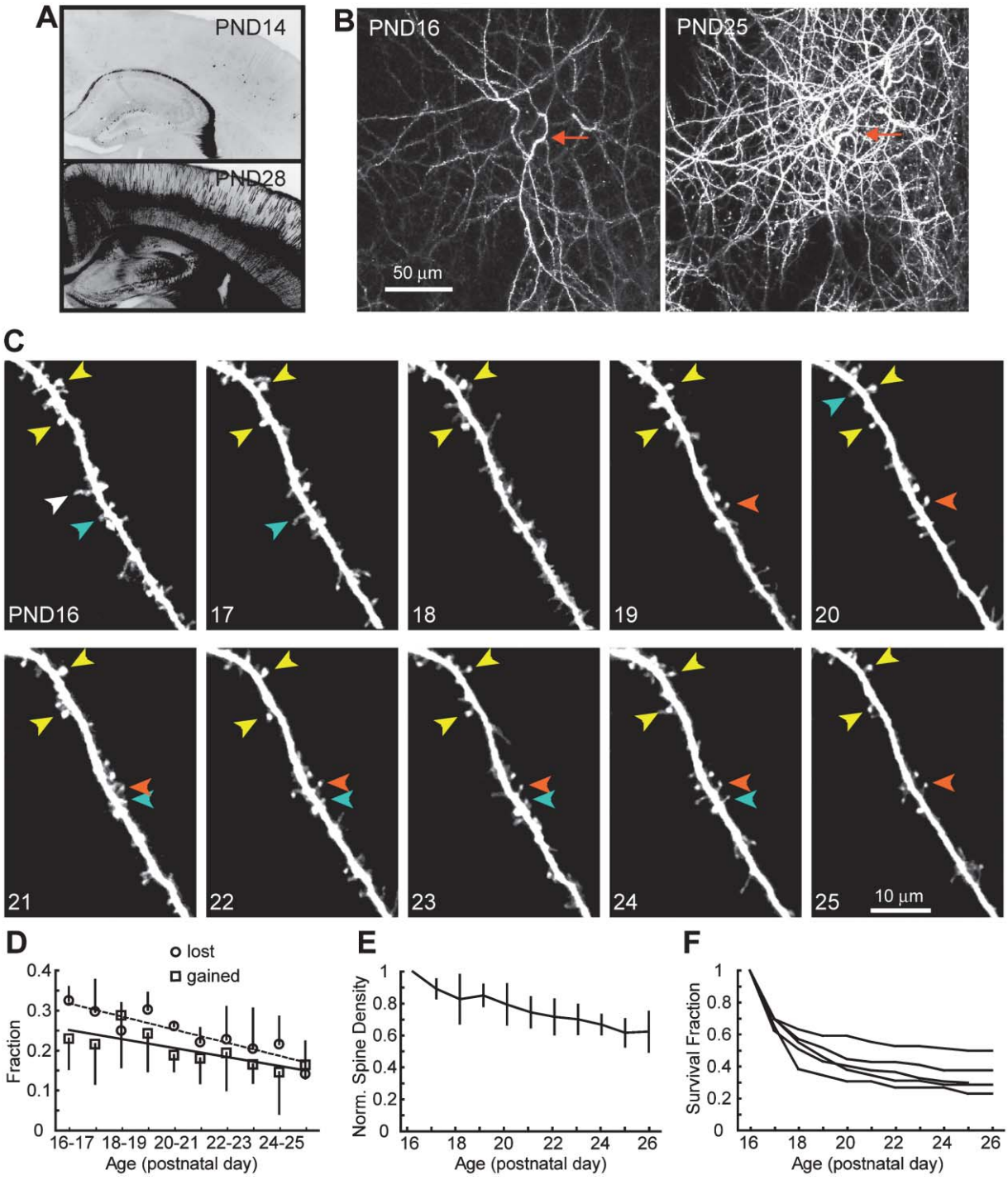

Figure 1. Transient and Persistent Spines during Development in S1

(A) Coronal sections from two YFP-H mice (top, PND 14; bottom, PND 28) showing developmental regulation of YFP expression in S1 (inverted contrast). In S1, expression is brightest in L5B at all ages.

(B) Dendritic arbors in a YFP-H animal at PND 16 and PND 25 (projection of 60 sections collected with 3 μm spacing). Bright dendrites belonging to one cell stand out, but several dim dendrites and axons are also apparent. The red arrow points to the same branch point at both ages.

(C) Time-lapse image of a dendritic branch (PND 16–25). Note the presence of persistent spines (e.g., yellow arrowheads), spines that appear and disappear over the imaging period (transient spines, e.g., blue arrowheads; new persistent spines, e.g., red arrowhead), and filopodium-like structures (e.g., white arrowhead).

(D) Fraction of spiny protrusions gained (squares) or lost (circles) from day to day as a function of age.

(E) Normalized spine density as a function of age.

(F) Survival function of spines in individual cells.

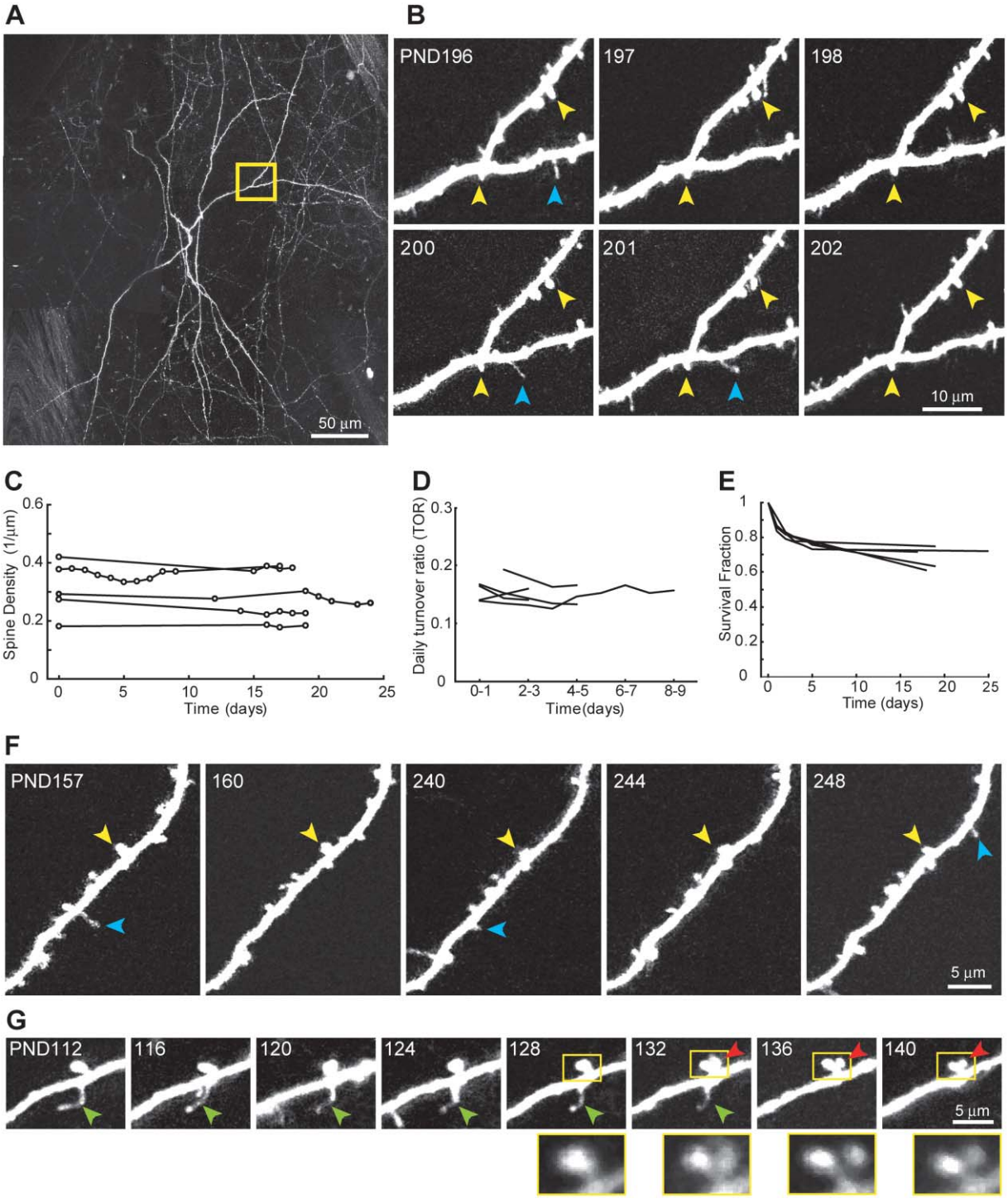

Figure 2. Transient and Persistent Spines in S1 of Mature Adult Mice

(A) Low-magnification image (montage) of a L5B dendritic arbor in S1 of a 6-month-old GFP-M mouse (projection of 88 sections; 3 µm spacing).

(B) Time-lapse image of a dendritic branch (from boxed region in [A]). Note the presence of persistent (e.g., yellow arrowheads) and transient spines (e.g., blue arrowheads).

(C) Spine densities. Lines correspond to individual cells, and circles indicate imaging days.

(D) Daily turnover ratios: the fraction of spines gained and lost from day to day. Lines correspond to individual cells.

(E) Survival function of spines in individual cells.

(F) Time-lapse image of a dendritic branch over 3 months. Transient spines appear and disappear throughout the entire imaging period (blue arrowheads).

(G) Time-lapse image (from a 3-month-old mouse) showing a thin persistent spine (green arrowhead) and a new persistent spine (red arrowhead). The thin spine was imaged for 20 days before it was lost. The new spine (red arrowhead) persisted for at least 8 days. (Bottom) The spines in the boxed region are shown in separate images with less contrast.

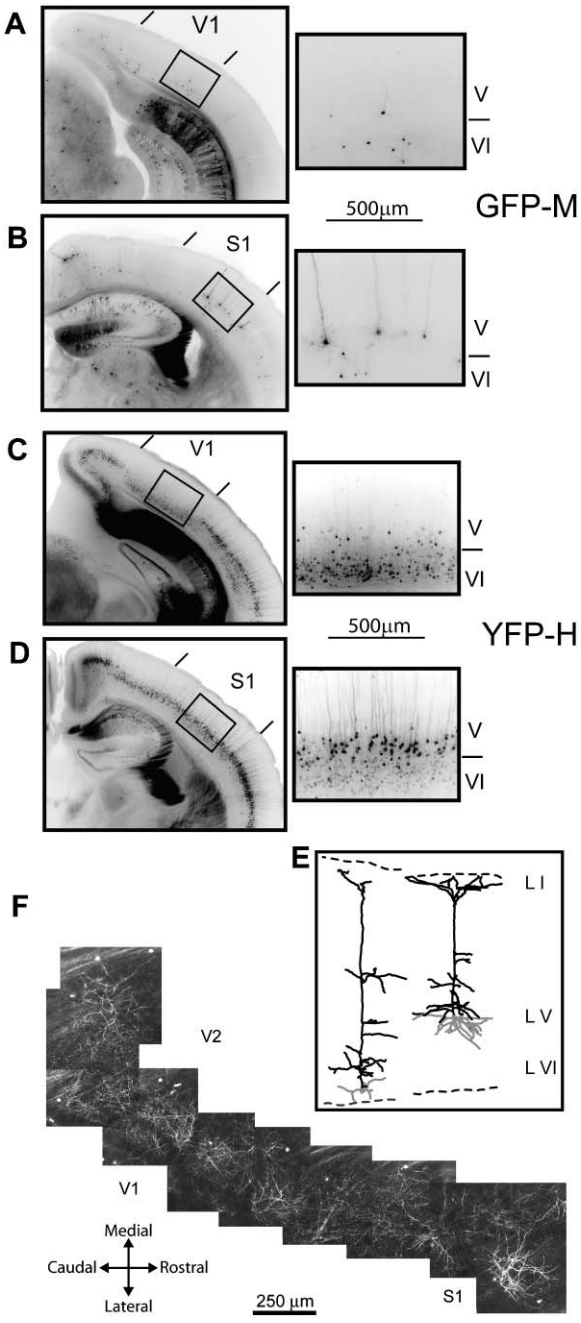

Figure 3. Expression of Fluorescent Proteins in the Primary Visual and Somatosensory Cortices of GFP-M and YFP-H Mice

(A–D) Different cell types express fluorescent proteins in the primary visual and somatosensory cortex. (A and C) Coronal sections through V1 in an adult GFP-M and YFP-H mouse, respectively, showing that mostly L6 neurons are labeled (inverted contrast). Compared to L5B, L6 has a high density of small somata (Braitenberg and Schutz, 1991). (B and D) Sections through S1, showing mostly labeled L5B neurons.

(E) Typical dendritic morphologies for L6 (left) and L5B (right) neurons with apical tufts in layer 1 and 2 (gray, basal dendrites; black, apical dendrites).

(F) In vivo image of dendrites of L5B neurons in S1 and visual cortex (V2) in a GFP-M mouse imaged in vivo (montage of several image stacks).

The transient spine density was also significantly lower in 6-month-old mice compared to young adult mice ($0.060 \pm 0.017\ \mu m^{-1}$ versus $0.117 \pm 0.028\ \mu m^{-1}$; $p < 0.01$; Figure 6B).

We further imaged dendritic spines in mice at an intermediate age (3 months; $n = 7$; 2287 spines). At this age, the fraction and density of transient spines ($24.2\% \pm 6.5\%$; $n = 7$), as well as the fraction of persistent spines ($66.4\% \pm 11.5\%$; $n = 3$), were intermediate (Figures 6A and 6B), indicating that spine stability increases gradually with age.

Spine Plasticity and Stability in the Visual Cortex

Previous in vivo imaging studies in mice revealed largely persistent spines in the adult (>4 months) visual cortex (VC) (Grutzendler et al., 2002), while a considerable fraction of spines is transient in young adult (2 months) S1 (Figure 6) (Trachtenberg et al., 2002). The age difference of the animals used in the published studies may explain part of this discrepancy (Figure 6A). However, significant differences remain: Grutzendler et al. claim more than 90% of persistent spines over a month of imaging in VC, while our measurements give 73% in S1 (Figures 2E and 6A). One interesting possibility is that these differences could reflect differences in plasticity in S1 and VC (Daw et al., 1992; Fox, 1992). Alternatively, differences could be due to methodological factors, such as housing, handling, or genotype of the animals, the cell types analyzed, sampling of cell types and dendritic branches, experimental preparation, and analysis criteria. Control experiments revealed that handling and housing conditions are not likely to play a major role in determining spine turnover (see the Supplemental Data at http://www.neuron.org/cgi/content/full/45/2/279/DC1/; Supplemental Figures S4 and S5). To test for differences between S1 and VC, we measured spine structural plasticity in methodologically identical experiments.

Comparing structural plasticity in VC and S1 is complicated by the fact that different populations of neurons tend to be labeled in VC and S1 (Figures 3A–3D). This can be easily visualized in coronal sections from YFP-H animals (Figures 3C and 3D). In S1, the majority of brightly labeled cells are in L5B (Figure 3D), with some labeling of L6 and L2/3 cells. In V1, mostly L6 neurons are labeled (Figure 3C) (Braitenberg and Schutz, 1991; De No, 1992). The same spatial pattern holds for GFP-M animals (Figures 3A and 3B). L5B neurons have tufts in L1 and L2 (Trachtenberg et al., 2002; Zhu, 2000), but so do L2/3 cells and a subpopulation of labeled L6 neurons (Katz, 1987) (Figure 3E). The presence of dendrites in L1 therefore does not suffice to identify the cell type. However, since profound laminar differences in physiological plasticity are typical (Daw et al., 1992; Diamond et al., 1994; Fox, 1992), laminar differences in structural plasticity are also likely (Figure 5), and identifying the cell type is important. It is further essential that identical cell types are studied when comparing structural plasticity in different brain regions. Here, we limited ourselves to L5B pyramidal neurons, confirmed in 3D reconstructions (Figure 3E). Since L5B neurons centered on V1 were rare, we also included in the analysis L5B cells in V2 (Figure 3F and 4A).

Time-lapse imaging studies in the VC of 3- to 6-month-old mice ($n = 6$; 1092 spines) revealed that a subpopula-

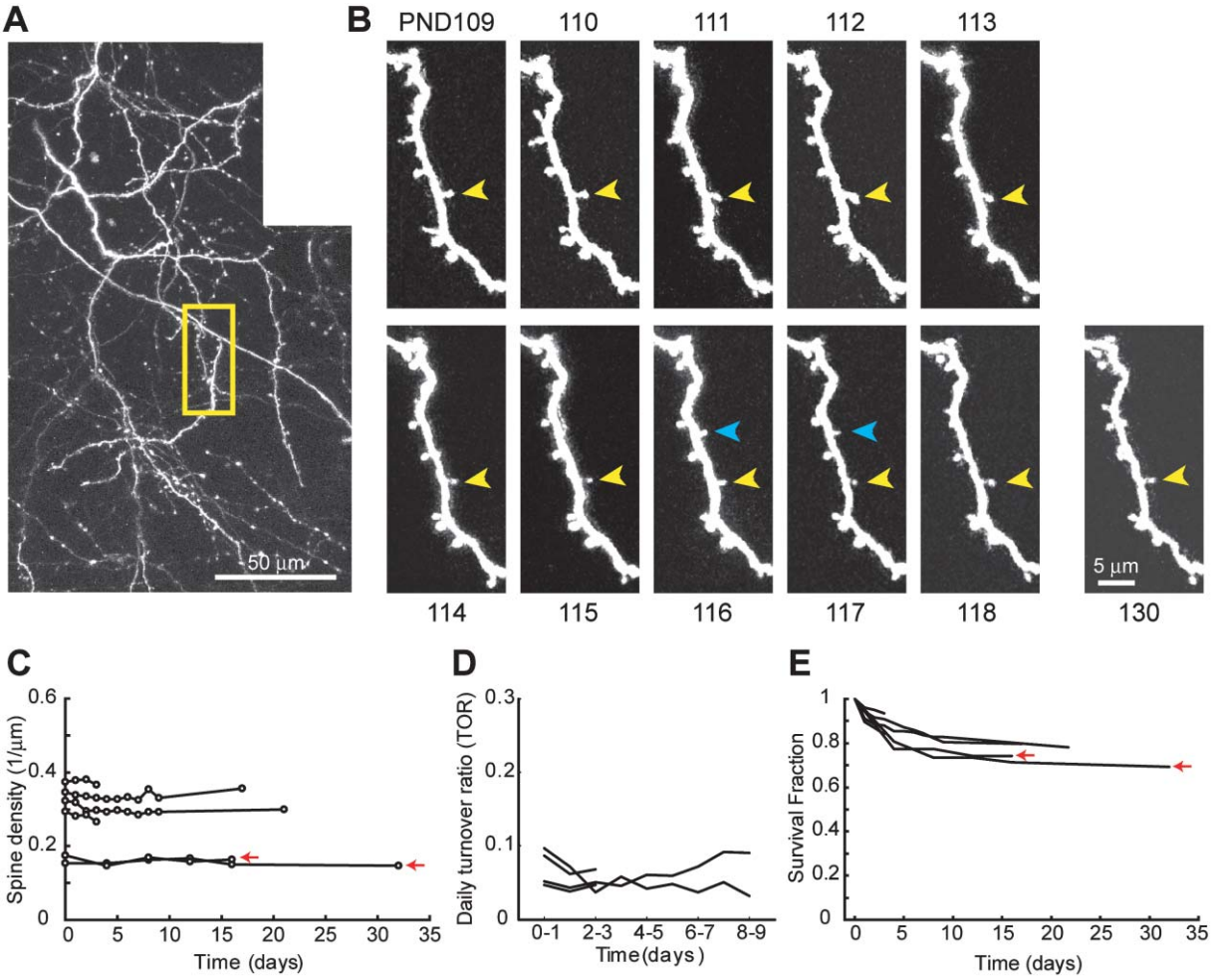

Figure 4. Transient and Persistent Spines in the Visual Cortex of Mature Adult Mice

(A) Low-magnification image (montage) of a L5B dendritic arbor in V2 of a 3-month-old GFP-M animal (projection of 82 sections; 3 μm spacing).

(B) Time-lapse image of a dendritic branch (from boxed region in [A]). Note the presence of persistent spines (e.g., yellow arrowheads) and transient spines (e.g., blue arrowheads).

(C) Spine densities. Lines correspond to individual cells, and circles indicate imaging days.

(D) Daily turnover ratios.

(E) Survival function of spines in individual cells. Note that the two dendrites with a relatively high fraction of transient spines (red arrows) have low spine densities (red arrows in [C]; see also Figure 6C).

tion of spines appeared and disappeared from day to day (Figure 4B), while spine densities were stable (Figure 4C). These data are qualitatively similar to the data from S1 (Figure 2B). However, the rate of spine addition and subtraction was significantly lower in VC than in S1 (TORs: VC, 5.7% ± 1.1%, n = 4; S1, 15.4% ± 1.6%, n = 5; $p < 0.001$) (cf. Figures 2D and 4D). The fraction of transient spines (lifetimes ≤ 4 days) was also lower in VC than in S1 (11.7% ± 5.9%, n = 6 versus 21.4% ± 4.3%, n = 5; $p < 0.05$) (cf. Figures 2E and 4E), as was the density of transient spines (0.028 ± 0.006 μm^{-1} versus 0.060 ± 0.017 μm^{-1}; $p < 0.01$) (Figure 6B). These differences were apparent in measurements in S1 and VC in the same animal (Supplemental Figure S2B at http://www.neuron.org/cgi/content/full/45/2/279/DC1/). Similarly, the fraction of VC spines that were persistent over 8 days was significantly higher than in that S1 (78.9% ± 4.4%, n = 4 versus 72.5% ± 2.6%, n = 5; $p < 0.05$). However, this difference disappeared over longer intervals: the survival fraction for more than 16 days was not significantly different (VC, 75.8% ± 1.5%; S1, 68.5% ± 6.1%; $p > 0.05$; cf. Figures 2E and 4E; Figure 6A) and was also lower than previously reported (Grutzendler et al., 2002). These data imply that spines turn over more rapidly in S1 than VC, but that long-term persistence is not significantly different in VC than in S1.

Similar to S1, the spine densities in VC varied greatly from cell to cell (range 0.15–0.38 μm^{-1}), and so did the fraction of transient spines (range 6%–22%). Similar to S1, in the VC there was a significant inverse correlation (analysis of variance [ANOVA], $p < 0.05$) between the total spine density and the fraction of transient spines (Figures 4C and 4E, arrows; Figure 6C), so that the density of transient spines was independent of the total spine density (data not shown). This suggests that the potential for structural spine plasticity is constant per

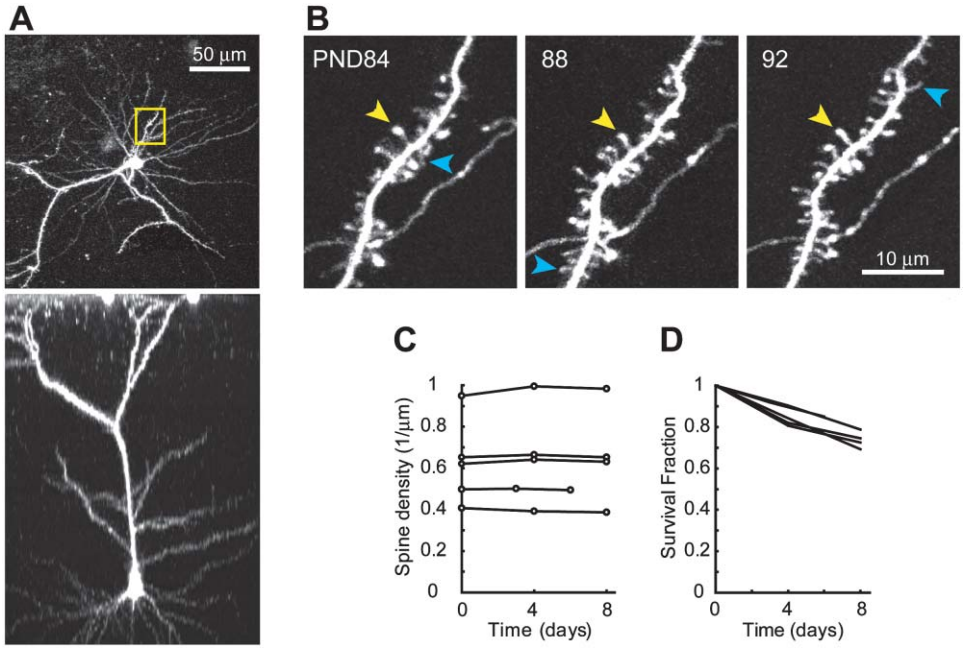

Figure 5. Transient and Persistent Spines of L2/3 Pyramidal Cells in S1

(A) Low-magnification image of a L2/3 neuron in S1 of a GFP-M mouse (top panel, projection of 95 sections, 3 μm spacing; bottom panel, side view). The cell body is located at ~280 μm below the dura.

(B) Time-lapse image of a dendritic branch (from boxed region in [A]). Note the presence of persistent spines (e.g., yellow arrowheads) and transient spines (e.g., blue arrowheads).

(C) Spine densities. Lines correspond to individual cells, and circles indicate imaging days.

(D) Survival function of spines in individual cells over 6–8 days.

dendritic length and that less spiny neurons may be relatively more plastic.

Spine Plasticity and Stability in L2/3 Neurons

Receptive field plasticity in the adult cortex depends on laminar location (Daw et al., 1992; Diamond et al., 1994; Fox, 1992). In a small fraction of GFP-M mice ($n = 5$), L2/3 neurons were labeled in S1, allowing us to compare spine stability and plasticity in the apical tufts of L5B and L2/3 neurons. L2/3 neurons have less elaborate tufts in L1/2 than L5B neurons (Figure 5A), but their dendrites are studded with much higher densities of dendritic spines (range 0.4–1 μm^{-1}) (Figures 5B and 5C). We tracked the fates of spines ($n = 5$; 1331 spines; age 3–6 months) in time-lapse images acquired every 4 days. A subpopulation of spines appeared and disappeared between imaging sessions. We detected small quantitative differences between L5B and L2/3 (cf. Figures 5D and 2E). To compare L5B and L2/3 cells, we grouped all animals that were 3 months or older for both cell types ($n = 12$ for L5B in S1; $n = 5$ for L2/3 in S1). The density of transient spines was higher in L2/3 than in L5B cells (0.102 ± 0.051 μm^{-1} versus 0.063 ± 0.019 μm^{-1}; $p < 0.05$) (Figure 6B). However, due to the higher spine density in L2/3, the fraction of transient spines was lower in L2/3 than in L5B cells (15.5% ± 3.9% versus 23.0% ± 5.6%; $p < 0.05$).

Transient Spines Are Thin

Our data suggest that, under conditions of stable sensory input, spines are either transient or persistent. During development, the fraction of persistent spines increased while the fraction and density of transient spines decreased (Figures 6A and 6B). We tested for morphological differences between transient and persistent spines of L5B neurons of mature adult mice. Cortical spines are highly heterogeneous, varying in volume by two orders of magnitude or more (Harris et al., 1992; Vaughn and Peters, 1973). Control experiments show that our microscopic technique has sufficient sensitivity to detect even the smallest spines (Supplemental Data; Supplemental Figure S3 at http://www.neuron.org/cgi/content/full/45/2/279/DC1/) (Chen et al., 2004). Because spine sizes are often smaller than the resolution limit of optical microscopy, morphometric parameters are difficult to estimate by measuring distances alone. To classify spines, we use as a measure of spine size the integrated fluorescence intensity generated by spines projecting laterally from dendrites ("spine brightness"). Assuming homogeneous filling of the cytoplasm with fluorescent protein, the spine brightness is expected to be proportional to the fraction of spine volume accessible to the fluorophore (Svoboda et al., 1996).

Some spines that were imaged in vivo (14 spines) were subsequently reconstructed using serial section electron microscopy (SSEM) (Trachtenberg et al., 2002) (Figure 7A, left). This confirmed our qualitative in vivo classification of spine shapes. In addition, the volume and surface area of the SSEM-reconstructed spines was used to test whether spine brightness is a good measure of spine size. In our sample, spine volumes ranged from

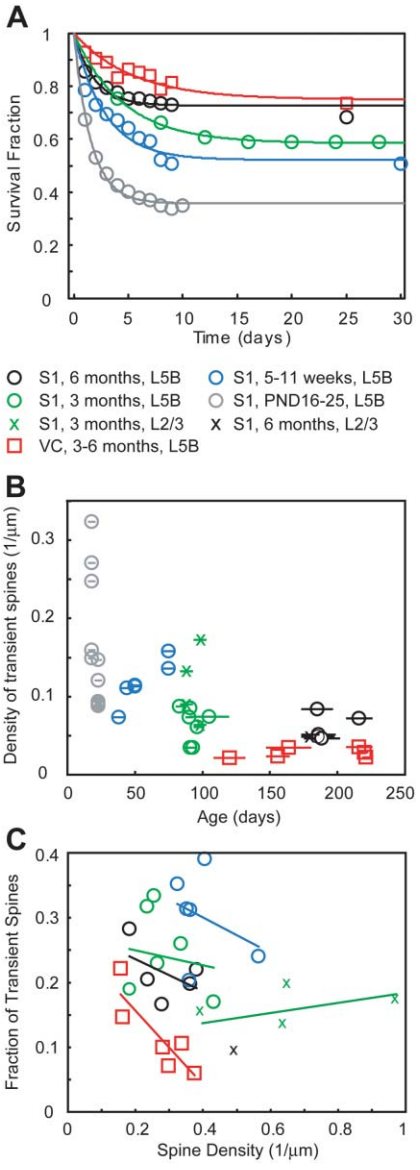

Figure 6. Summary of Spine Turnover and Stability

(A) Averaged SFs (circles) were fit with an exponential and constant term, $SF = fe^{-t/\tau} + s$ (lines). The fit serves to guide the eye and as an estimate of the persistent (s) and transient (f) spine fraction. The fit parameters are as follows (time constant, τ in days; persistent fraction, s; $f = 1 - s$): red, $\tau = 5.4$, $s = 0.75$; black, $\tau = 1.9$, $s = 0.73$; green, $\tau = 4.5$, $s = 0.58$; blue, $\tau = 2.9$, $s = 0.52$; gray, $\tau = 1.6$, $s = 0.36$. The data from S1, 5–11 weeks (blue), are from Trachtenberg et al. (2002).

(B) Density of transient spines (lifetime $\leq$ 4 days) as a function of age. The horizontal lines through the data points represent the period over which the animal was imaged. Each data point represents a cell. Note the decrease in transient spine density with age and the lower transient spine density in VC compared to S1 at all ages.

(C) The fraction of transient spines as a function of spine density. L5B cells with low spine densities tend to have a higher fraction of transient spines. The inverse correlation between spine density and the fraction of transient spines is significant (ANOVA, $p < 0.05$) in the VC.

0.005 μm^3 to 1.1 μm^3, and spine brightness increased monotonically with volume (Figure 7A, right). Curiously, spine brightness was more closely proportional to spine surface area rather than spine volume (line in Figure 7A, right). This scaling relationship may be related to different fractions of excluded volume in spines of different sizes, perhaps because of volume occupied by the spine apparatus and other organelles (Spacek, 1985), or affinity of fluorescent proteins for spine membranes. Nevertheless, it is clear that spine brightness is a good measure of spine size.

In a representative sample of spines imaged in vivo (Experimental Procedures), we characterized spine morphologies by plotting spine brightness against spine length (Figure 7B). Spine brightness varied by two orders of magnitude, reflecting the heterogeneity of spine sizes. Correlating morphology with dynamics measured in vivo revealed that the majority of spines that turned over had small volumes; many were long and thin (Figure 7B, left). However, this distinction was not absolute, since some thin spines persisted for extended periods (Figure 2G, green arrowhead). Comparing morphologies from S1 and VC further revealed that long, thin spines (spine length > 1.5 μm; rel. spine brightness < 0.4) were more likely to occur in S1 than in the VC (17% $\pm$ 3% in S1 versus 9% $\pm$ 2% in VC; $p < 0.05$; binomial statistics; Figure 7B).

We measured the time course of spine brightness of a subset of transient spines and compared them with persistent spines on the same dendrite (Figure 7D, left). Transient spines remained thin (dim) over the entire period of their existence, while persistent spines were consistently thick (bright). The lengths of transient spines were dynamic, possibly indicating that they were in a mode of growth (Figure 7D, right), while the length of persistent spines was relatively constant. These observations lend support to the notion that transient and persistent spines constitute largely independent populations and that there is little interchange between them under our experimental conditions.

We tested if the small volume spines associated with high turnover are also observed in tissue that had not been previously imaged in vivo. The morphologies of spines imaged in vivo were compared to spines imaged in naive perfusion-fixed brain (Figure 7C, left). The distributions of morphologies in vivo and in fixed tissue were indistinguishable (Figure 7C, right; $p > 0.2$, ANOVA; Experimental Procedures). Small-volume spines occurred in fixed tissue with similar incidence to the intact brain in vivo (Figure 7C) and therefore were not induced by imaging. As in the intact brain in vivo, in fixed tissue a larger fraction of spines were classified as long and thin in S1 compared to VC (18% $\pm$ 5% in S1 versus 6% $\pm$ 3% in VC; $p < 0.05$). We conclude that transient spines are thin and suggest that the presence of thin spines (for example, in S1) predicts high levels of spine turnover.

Discussion

Which elements of neural circuits are plastic in the developing and the adult neocortex? And which elements are stable? To begin to address these questions, we imaged the apical tufts of neocortical pyramidal neurons during

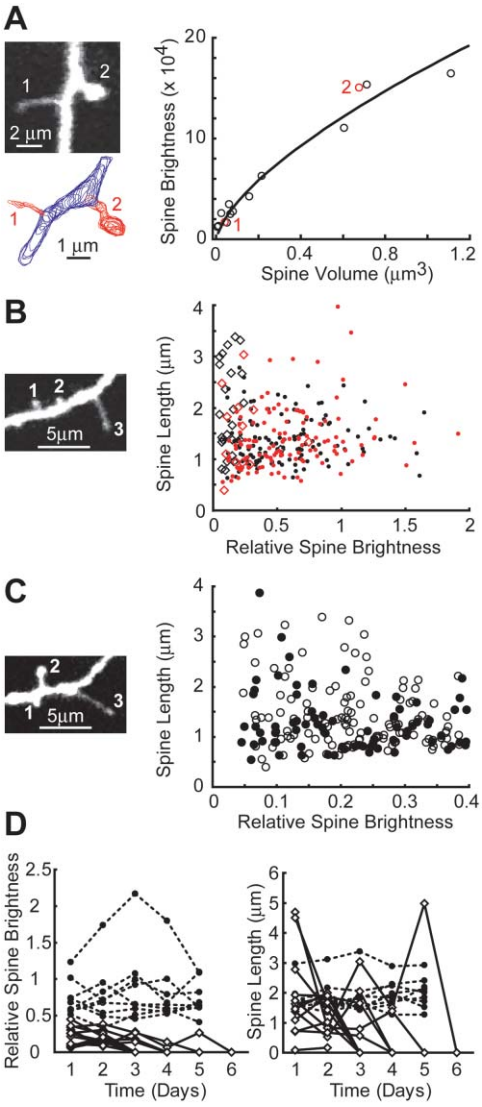

Figure 7. Morphological Analysis of Dendritic Spines

(A) (Left) Dendritic spines that had been imaged in vivo and then reconstructed with serial section electron microscopy. (Right) Spine brightness (fluorescence intensity integrated over a dendritic spine − background intensity) as a function of spine volume, *V*. The line is the best fit to the function $cV^{2/3}$. Numbered symbols correspond to the images in the left column.

(B) (Left) In vivo image. (Right) Spine morphologies in vivo (black, S1; red, visual cortex). Spine brightness was normalized by dendritic brightness (Experimental Procedures). Diamonds indicate transient spines that disappeared in vivo. Spines numbered in the left panel correspond to the following values: 1 (0.21, 1.1); 2 (0.20, 0.7); 3 (0.11, 3.3).

(C) (Left) Image in perfusion-fixed tissue. (Right) Comparison of spine morphologies imaged in vivo (open circles) and in fixed naive cortex (solid circles). Note that the horizontal axis was stretched compared to (B). The distributions were not different ($p > 0.2$; Experimental Procedures). Spines numbered in the left panel correspond to the following values: 1 (0.25, 0.8); 2 (0.65, 2.1); 3 (0.07, 3.9).

(D) A subset of transient spines with a lifetime ≥ 2 days (diamonds, solid lines) and persistent spines (circles, dashed lines) was followed for 5 days. All spines are neighboring spines on the same L5B cell in S1. (Left) Relative spine brightness as a measure of volume over time. Note that transient spines remain thin throughout their existence, while persistent spines are persistently thick. (Right) Spine length of the same subset of spines over time. Transient spines vary greatly in length during their existence; persistent spines remain constant in length.

development and in the adult under conditions of constant sensory experience. While the branching of dendritic arbors was stable (Mizrahi and Katz, 2003; Trachtenberg et al., 2002), a fraction of spines appeared and disappeared over timescales of days. The other spines persisted for weeks, and this persistent fraction grew gradually during development and in the adult, providing evidence that synaptic circuits continue to stabilize even in the mature brain. In the visual cortex, spines were found to turn over more slowly than in the primary somatosensory cortex (S1).

Persistent and Transient Spines in the Neocortex

Spines are motile structures. They can undergo morphological changes on timescales of seconds and minutes (Bonhoeffer and Yuste, 2002; Dailey and Smith, 1996; Fischer et al., 1998; Lendvai et al., 2000). Complete retraction and the novo sprouting can occur over hours and days (Dailey and Smith, 1996; Engert and Bonhoeffer, 1999; Lendvai et al., 2000; Maletic-Savatic et al., 1999; Trachtenberg et al., 2002). Our in vivo experiments provide evidence for shape changes as well as spine addition and subtraction over timescales of days (Figures 1, 2, and 4–7). Here, we have focused our analysis on spine addition and subtraction, since these processes may indicate synapse formation and elimination (Knott et al., 2002; Toni et al., 1999; Trachtenberg et al., 2002), a proposed substrate for experience-dependent reorganization of synaptic circuits in the adult brain (Lendvai et al., 2000; Trachtenberg et al., 2002; Turner and Greenough, 1985) (Figure 8).

Time-lapse imaging of individual spines has revealed kinetically distinct populations of dendritic spines at all developmental ages. This can be seen in the shape of the survival function (i.e., the fraction of spines that survive over time) (Figure 6A). A fraction of spines, *f*, appear and disappear over a few days (transient spines; typically ≤4 days). At the same time, a complementary fraction of spines, $s = (1 - f)$, is remarkably persistent. Under our experimental conditions, most spines that appear survive for at most a few days. Spines that appear and persist are rare (Figures 1C and 2G and Supplemental Figure S2C [http://www.neuron.org/cgi/content/full/45/2/279/DC1/], red arrowheads). Similarly, spines that survive for 8 days are highly likely to survive for a month and longer (Figure 2F). Therefore, the persistent and transient fractions belong largely to independent populations with relatively little transfer between them (Figure 8).

We have further analyzed the morphology of dendritic spines with reference to their dynamic properties in vivo (Figure 7). Transient spines are small and thin, while persistent spines tend to be relatively thick, including classic mushroom-shaped spines (Harris et al., 1992; Peters and Kaiserman-Abramof, 1970). It is possible, however, that under some conditions, perhaps involving changing patterns of activity induced by novel sensory experience, thin spines bearing nascent synapses become stabilized and enlarged in response to salient synaptic stimuli (Matsuzaki et al., 2004).

Some transient spines are structurally similar to "dendritic filopodia" seen in young, growing dendrites (Dailey and Smith, 1996), but they are dynamically distinct: filo-

Figure 8. Schematic Relating the Turnover of Dendritic Spines and the Plasticity of Cortical Circuits

A spiny dendrite (green), connected axons (red), and unconnected axons (black) are shown. Under baseline conditions, addition and subtraction of thin, transient spines may contribute to temporary changes in connectivity in cortical circuits. Such spine turnover could therefore provide a means to promptly adapt the neuronal network to novel requirements. After novel sensory experience, a fraction of transient spines may be stabilized.

podia last for minutes (Dailey and Smith, 1996; Lendvai et al., 2000; Portera-Cailliau et al., 2003), while transient spines last for days. Transient spines are structurally similar to "thin spines" described in hippocampal tissue (Harris et al., 1992). Ultrastructural analysis reveals that both large and small spines can make synapses (Harris et al., 1992; Trachtenberg et al., 2002; Vaughn and Peters, 1973), but there could be functional differences between these synaptic populations. Large spines have large postsynaptic densities (Harris et al., 1992) and a larger number of AMPA-type glutamate receptors (AMPA-R) (Nusser et al., 1998). The distribution of AMPA-R proteins is strongly skewed toward large spines (Nusser et al., 1998), so that there is a small population of synapses, mostly at large mushroom-shaped spines, which contains very large numbers of AMPA-Rs (Matsuzaki et al., 2001). However, physiological (Nimchinsky et al., 2004) and immunoelectron microscopic data (Racca et al., 2000; Takumi et al., 1999) have shown that the number of NMDA receptors (NMDA-Rs) activated may be independent of spine size (Nimchinsky et al., 2004). Based on these studies (all in the hippocampus), it appears that small spines will tend to produce large NMDA-R- but small AMPA-R-mediated currents and may even be associated with postsynaptically silent synapses (Malinow and Malenka, 2002).

What could be the role of transient spines and their synapses in the plasticity of cortical circuits? Our data, together with previous studies (Trachtenberg et al., 2002), suggest the following model. New spines sample from the set of available presynaptic partners (potential synapses; Figure 8) (Stepanyants et al., 2002). Most new synapses are retracted and are therefore transient. In the presence of novel sensory experience, a fraction of synapses may be stabilized in an activity-dependent manner, perhaps associated with insertion of AMPA-Rs (Malinow and Malenka, 2002) and expansion of spine size (Matsuzaki et al., 2004). In this model, long-term changes in neural circuits associated with novel sensory experience would be encoded in new patterns of persistent spine synapses, while transient spines serve to facilitate circuit plasticity. Further experiments, combining long-term in vivo imaging with manipulations of sensory experience will be required to test this model.

Development of Spine Turnover and Stability in the Somatosensory Cortex

Spiny protrusions show large-scale (μm) motility during development in vitro (Dailey and Smith, 1996; Maletic-Savatic et al., 1999; Portera-Cailliau et al., 2003) and in vivo (Grutzendler et al., 2002; Lendvai et al., 2000; Majewska and Sur, 2003). The time course of these rearrangements slows down with developmental age, from minutes in young dendrites that are still elaborating (Dailey and Smith, 1996; Lendvai et al., 2000; Portera-Cailliau et al., 2003) to hours in recently stabilized dendrites (Lendvai et al., 2000; Maravall et al., 2004). Using time-lapse imaging, we tracked the developmental changes in spine plasticity from the third postnatal week into mature adulthood (Figures 1 and 2).

At the earliest ages imaged (PND 16), dendrites were studded with abundant dendritic spines. A large fraction (*f* 65%) of these spines disappeared within a few days. Remarkably, a substantial fraction of these early spines (*s* 35%) already persisted for almost 2 weeks and likely longer (Figure 1). Thus, the first persistent spines arise sometime before PND 16, perhaps coincident with dendritic stabilization and closure of critical periods (Lendvai et al., 2000). It is possible that the cell adhesion provided by large, persistent spine synapses is required to anchor dendritic branches (Niell et al., 2004).

Over the third and fourth week of life, spine density was not constant but decreased with developmental age (Figure 1). L5B tuft dendrites lost dendritic spines at a rate that exceeded the growth of new spines. This is surprising because excitatory synaptic densities in L1 are still growing over this developmental period in S1 (De Felipe et al., 1997). Our results suggest that this increase in synaptic densities is likely due to neurons not imaged here, such as L2/3 neurons, which are born after L5 neurons and hence constitute a less mature population. In addition, spine densities have been reported to increase in L5 neurons in visual cortex over the third and fourth week of life (Juraska, 1982). These results are also not inconsistent with our studies in S1, since V1 develops later than S1 (Fox, 1995), and the developmental differences in spine pruning in these brain areas likely reflect this fact.

Although spines appear and disappear at all developmental ages that we have probed, in S1 the persistent fraction (lifetime $\geq$ 8 days) increases with developmental age, from $\sim$35% at PND 16–25, to $\sim$54% for 5- to 11-week-old mice (Trachtenberg et al., 2002), $\sim$66% for 3-month-old mice, and $\sim$73% for 6-month-old mice (Figure 6). This provides evidence that the structure of synaptic circuits in the neocortex continues to stabilize gradually as animals mature from young adulthood to middle age, long after the closure of known critical periods in S1 (Fox, 1992; Stern et al., 2001). This observation is consistent with electrophysiological data showing that receptive field plasticity in the extragranular layers of S1 continues to decrease gradually over a similar range of ages (Fox, 2002). Late maturation of synaptic structural plasticity has also been observed in the visual cortex (Grutzendler et al., 2002) and the parasympathetic submandibular ganglion (Gan et al., 2003). In contrast, the neuromuscular junction stabilizes rapidly during the first 2 weeks of life and is remarkably constant

during adulthood (Lichtman et al., 1987; Walsh and Lichtman, 2003).

Spine Turnover and Stability in the Somatosensory and Visual Cortex

Direct comparison of L5B spines in S1 and VC (Figures 2, 4, and 6; Supplemental Figure S2 at http://www.neuron.org/cgi/content/full/45/2/279/DC1/) revealed that spines turn over more slowly in visual cortex than in somatosensory cortex. However, long-term (>2 weeks) persistence was not significantly different. Some quantitative differences remain to be explained between our data and the study of Grutzendler et al. (2002). In the VC of 6-month-old mice, Grutzendler et al. find >90% persistent spines over 1 month of imaging, while our number is ~75% (Figures 4E and 6A). This difference could be explained by a combination of the following factors. (1) Grutzendler et al. imaged dendrites in YFP-H animals without identifying the cell type. It is possible that in their study, neurons other than L5B cells were imaged and that these have more stability than the L5B neurons imaged here. (2) Another difference may involve sampling. In our study, we randomly sampled the dendritic tuft of individual GFP-expressing L5B or L2/3 cells, irrespective of spine density. Selection of highly spiny branches would lead to a substantial underestimate of plasticity (Figure 6C). (3) The imaging window preparation we use allows detection of all spines, including the smallest structures that are most likely to be transient (Supplemental Data [http://www.neuron.org/cgi/content/full/45/2/279/DC1/]). It is possible that imaging through the thinned skull does not allow the detection of the smallest spines, which could have a profound impact on the rate of measured spine turnover (Figure 7B). For example, consider a subset of spines imaged in vivo that were also analyzed for spine volume (Figure 7B). If we ignore the dynamics of the dimmest 15% of spines, we find only 5% transient spines, in line with Grutzendler et al.

The difference in the rate of turnover of spines in S1 and VC may be related to differential use of the corresponding sensory modalities within the limited environment of the laboratory cage. Alternatively, the differences may reflect the potential for physiological plasticity in these brain regions. The latter view is consistent with physiological studies of experience-dependent plasticity in the adult brain in vivo. Whisker dominance plasticity in the barrel cortex and ocular dominance plasticity in the visual cortex are analogous paradigms for the induction of competitive experience-dependent circuit modifications in these different brain regions. In the extragranular layers of S1, whisker dominance plasticity is rapidly (1–2 days) inducible (Barth et al., 2000; Diamond et al., 1994; Trachtenberg et al., 2002), while in the adult visual cortex prolonged (5 days) deprivation is required (Sawtell et al., 2003). These timescales of plasticity match the time constants of the spine survival functions in these brain areas (Figure 6A).

Experimental Procedures

Surgery

Male c57/Bl6 transgenic mice (PND 14 to PND 511) in which a Thy-1 promoter drives the expression of XFP (GFP, line M; YFP, line H) (Feng et al., 2000) in a subset of cortical neurons were used for this study. For surgery, mice were deeply anesthetized with an intraperitoneal injection of a ketamine/xylazine mixture (0.13 mg ketamine/0.01 mg xylazine/g body weight). A small dose of dexamethasone (0.02 ml at 4 mg/ml; prior to the surgery) was administered to minimize potential swelling at the surgical site and accumulation of fluid in the trachea in the anesthetized animal. The skull overlying the right barrel cortex was removed, leaving the dura intact. The dura was covered by a thin layer of low-melting point agarose (Sigma #A9793 1.5% in HEPES-buffered artificial cerebrospinal fluid) and a custom-made cover glass (No. 1), sealed in place with dental acrylic. Imaging began after a 10 day rest period, except for the developing animals (PND 16; Figure 1), where imaging began right after surgery. Between imaging sessions, animals were housed with same-sex littermates, typically three to five per cage, in plastic cages of dimensions 10L × 10W × 5H (inches). To promote whisking and exploration, cages were furnished with tubes consisting of high-density wire mesh, a small platform with evenly spaced coarse perforations, and a plastic tube with smooth walls.

Imaging

For imaging sessions, animals were anesthetized with ketamine/xylazine at ~2/3 surgical dose (see above). At this level, anesthesia typically wore off within 45–60 min, at which time animals were again returned to their cage. In vivo images of XFP-expressing neurons were acquired with a custom-built 2PLSM (Lendvai et al., 2000). As a light source, we used a Ti:sapphire laser (Tsunami, Spectra Physics), running at λ ~910 nm, pumped by a 10 W solid state laser (Millenia X, Spectra Physics). The objective (40×, 0.8 NA) and scan lens were from Zeiss, the trinoc was from Olympus, and the photomultiplier tube was from Hamamatsu. Detection optics with large apertures provided for optimal fluorescence detection (Oheim et al., 2001). Image acquisition was achieved with custom software (MatLab) (Pologruto et al., 2003).

In each animal, the apical dendritic tufts of pyramidal neurons in L5B or L2/3 (typically one per animal) were imaged over periods of 3–150 days. L5B corresponds to the lower ~1/2 of L5, distinguished by large cell bodies and a dark appearance in Nissl stains (Braitenberg and Schutz, 1991). The same cells were located each day using the unique vascular pattern in the region of the cell to grossly position the objective to within 100 μm, and then using fluorescence imaging to identify the cell by the unique branching pattern of its apical dendrites. For high-magnification spine imaging, 7 to 15 fields, each 50 × 50 μm, containing second and higher order branches (Juraska, 1982), were selected for each cell. Image stacks consisted of sections (512 × 512 pixels; 0.09 μm/pixel) collected in 1 μm steps. In addition, low-magnification images were collected (512 × 512 pixels; 0.3 μm/pixel; 3 μm steps). Care was taken to achieve close to identical fluorescence levels across imaged regions and imaging sessions. Imaged dendrites were within 100 μm from the surface of the brain and therefore in L1. All images in the figures are projections of 3D stacks. In some figures, distracting fluorescent processes were digitally removed from the images (Figure 1). Retrospective reconstructions of dendritic arbors and serial section electron microscopy was performed as described (Trachtenberg et al., 2002).

Analysis

For this study, a total of 6918 spines were tracked in time-lapse images (3 to 11 time points) using custom software. Imaging tiny structures, such as dendritic spines, has certain limitations. Because of the numerical aperture of long working distance, water immersion objectives, the resolution of our 3D images is insufficient to resolve spines reliably in the axial dimension. We have therefore not analyzed structures that projected mainly along the optical axis, below or above the dendrite. All clear protrusions emanating laterally from the dendritic shaft, irrespective of apparent shape, were measured. Analysis was done blind, with the analyzer unaware of the experimental condition (i.e., cortical region or developmental age). For each day of each region, images were aligned with each other using fiducial marks, such as dendritic branch points, that were stable across all imaging days. Images were analyzed in three dimensions

for the presence or absence and length of each spine. Scoring spine addition and subtraction was based on the following criteria: spines were considered lost if they disappeared into the haze of the dendrite (length < 5 pixels); spines were gained if they clearly protruded from the dendrite (length ≥ 5 pixels). These criteria were robust, since three independent analyzers scored spine turnover similarly to within ~10% (seven regions, eight time points, two animals).

Turnover ratios, the fraction of spines appearing and disappearing from day to day, were calculated as TOR = $(N_{gained} + N_{lost})/(2 \times N_{total})$. The time-dependent survival function was calculated as $SF(t) = N(t)/N_o$, where N_o is the number of spines at $t = 0$, and $N(t)$ is the number of spines of the original set surviving after time t. By definition, $SF(t)$ is a monotonically decreasing function of time, and $SF(0) = 1$. Furthermore, $[1 - SF(1)] \approx$ TOR. To derive the persistent (s) and transient (f) spine fractions, SFs were fit with $SF = fe^{-t/\tau} + s$ (Figure 6). For statistical comparisons between groups, we defined the transient population as spines that lived for 4 days or less and the persistent population as spines that lived for 8 days or more. For four mice in the 6-month-old group, the 8 day survival fraction was derived through linear interpolation. n is the number of cells per group (typically equal to the number of animals). Errors in text and figures are given as standard deviation, unless noted otherwise.

To calculate spine brightness (Figure 7), the pixel values containing the spine head were summed. Background fluorescence, calculated over the same-sized box adjacent to the spine, was subtracted. Since dendritic shaft diameters were constant and relatively uniform, we used them to correct fluorescence levels for possible inhomogeneities in excitation level. For each imaged dendritic region (30–45 μm), average "shaft" pixel intensity was calculated. The background-subtracted, summed pixel value for each spine was divided by the average summed shaft pixel value. The resulting relative brightness is expected to be proportional to the accessible spine volume.

Comparison of Spine Structure In Vivo and in Fixed Tissue

To analyze spines and fluorescent protein expression in the naive brain with an intact skull, we perfused GFP-M (n = 3; 6 months old) and YFP-H mice (n = 17; ages PND 16–33; 6 months old) transcardially with 4% paraformaldehyde (pH = 7.4 in sodium phosphate). After perfusion, the skull was removed, and dendrites and dendritic spines were imaged under identical conditions to in vivo imaging (optics, magnification, orientation). For 107 randomly selected spines, we measured the spine length and brightness (integrated intensity). Similar measurements were made for randomly selected spines imaged in vivo (150 spines in S1; 136 in VC). An ANOVA showed no significant differences in brightness ($p > 0.2$) between the fixed and in vivo pools. Similarly, Monte Carlo simulations showed that the pools of spines imaged in naive, fixed tissue and in vivo are not significantly different in their length/brightness distributions.

Acknowledgments

We thank Brian Chen and Barry Burbach for help with experiments; Vincenzo De Paola, Carlos Portera, Karen Zito, and Egbert Welker for comments on the manuscript; and Josh Sanes for the GFP-M mice. This work was supported by the Netherlands Institute for Brain Research (AH); the Swiss National Foundation (GK); NIH; and HHMI.

Received: February 12, 2004
Revised: August 4, 2004
Accepted: December 30, 2004
Published: January 19, 2005

References

Antonini, A., and Stryker, M.P. (1993). Rapid remodeling of axonal arbors in the visual cortex. Science *260*, 1819–1821.

Barth, A.L., McKenna, M., Glazewski, S., Hill, P., Impey, S., Storm, D., and Fox, K. (2000). Upregulation of cAMP response element-mediated gene expression during experience-dependent plasticity in adult neocortex. J. Neurosci. *20*, 4206–4216.

Bonhoeffer, T., and Yuste, R. (2002). Spine motility. Phenomenology, mechanisms, and function. Neuron *35*, 1019–1027.

Braitenberg, V., and Schutz, A. (1991). Anatomy of the Cortex, Volume 18 (Berlin: Springer Verlag).

Callaway, E.M., and Katz, L.C. (1993). Photostimulation using caged glutamate reveals functional circuitry in living brain slices. Proc. Natl. Acad. Sci. USA *90*, 7661–7665.

Chen, B., Trachtenberg, J.T., Holtmaat, A.J., and Svoboda, K. (2004). Long-term, high-resolution imaging in the neocortex in vivo. In Live Cell Imaging, R.D. Goldman and D.L. Spector, eds. (Cold Spring Harbor, NY: Cold Spring Harbor Press), pp. 423–434.

Chklovskii, D.B., Mel, B.W., and Svoboda, K. (2004). Cortical rewiring and information storage. Nature *431*, 782–788.

Dailey, M.E., and Smith, S.J. (1996). The dynamics of dendritic structure in developing hippocampal slices. J. Neurosci. *16*, 2983–2994.

Darian-Smith, C., and Gilbert, C.D. (1994). Axonal sprouting accompanies functional reorganization in adult cat striate cortex. Nature *368*, 737–740.

Daw, N.W., Fox, K., Sato, H., and Czepita, D. (1992). Critical period for monocular deprivation in the cat visual cortex. J. Neurophysiol. *67*, 197–202.

De Felipe, J., Marco, P., Fairen, A., and Jones, E.G. (1997). Inhibitory synaptogenesis in mouse somatosensory cortex. Cereb. Cortex *7*, 619–634.

Denk, W., and Svoboda, K. (1997). Photon upmanship: why multiphoton imaging is more than a gimmick. Neuron *18*, 351–357.

Denk, W., Strickler, J.H., and Webb, W.W. (1990). Two-photon laser scanning microscopy. Science *248*, 73–76.

De No, R.L. (1992). The cerebral cortex of the mouse. Somat. Mot. Res. *9*, 3–36.

Diamond, M.E., Huang, W., and Ebner, F.F. (1994). Laminar comparison of somatosensory cortical plasticity. Science *265*, 1885–1888.

Engert, F., and Bonhoeffer, T. (1999). Dendritic spine changes associated with hippocampal long-term synaptic plasticity. Nature *399*, 66–70.

Feng, G., Mellor, R.H., Bernstein, M., Keller-Peck, C., Nguyen, Q.T., Wallace, M., Nerbonne, J.M., Lichtman, J.W., and Sanes, J.R. (2000). Imaging neuronal subsets in transgenic mice expressing multiple spectral variants of GFP. Neuron *28*, 41–51.

Fischer, M., Kaech, S., Knutti, D., and Matus, A. (1998). Rapid actin-based plasticity in dendritic spines. Neuron *20*, 847–854.

Fox, K. (1992). A critical period for experience-dependent synaptic plasticity in rat barrel cortex. J. Neurosci. *12*, 1826–1838.

Fox, K. (1995). The critical period for long-term potentiation in primary sensory cortex. Neuron *15*, 485–488.

Fox, K. (2002). Anatomical pathways and molecular mechanisms for plasticity in the barrel cortex. Neuroscience *111*, 799–814.

Gan, W.B., Kwon, E., Feng, G., Sanes, J.R., and Lichtman, J.W. (2003). Synaptic dynamism measured over minutes to months: age-dependent decline in an autonomic ganglion. Nat. Neurosci. *6*, 956–960.

Gilbert, C.D. (1998). Adult cortical dynamics. Physiol. Rev. *78*, 467–485.

Grutzendler, J., Kasthuri, N., and Gan, W.B. (2002). Long-term dendritic spine stability in the adult cortex. Nature *420*, 812–816.

Harris, K.M., Jensen, F.E., and Tsao, B. (1992). Three-dimensional structure of dendritic spines and synapses in rat hippocampus (CA1) at postnatal day 15 and adult ages: implications for the maturation of synaptic physiology and long-term potentiation. J. Neurosci. *12*, 2685–2705.

Juraska, J.M. (1982). The development of pyramidal neurons after eye opening in the visual cortex of hooded rats: a quantitative study. J. Comp. Neurol. *212*, 208–213.

Katz, L.C. (1987). Local circuitry of identified projection neurons in cat visual cortex brain slices. J. Neurosci. *7*, 1223–1249.

Katz, L.C., and Shatz, C.J. (1996). Synaptic activity and the construction of cortical circuits. Science *274*, 1133–1138.

Knott, G.W., Quairiaux, C., Genoud, C., and Welker, E. (2002). Formation of dendritic spines with GABAergic synapses induced by whisker stimulation in adult mice. Neuron *34*, 265–273.

Lendvai, B., Stern, E., Chen, B., and Svoboda, K. (2000). Experience-dependent plasticity of dendritic spines in the developing rat barrel cortex *in vivo*. Nature *404*, 876–881.

Lichtman, J.W., Magrassi, L., and Purves, D. (1987). Visualization of neuromuscular junctions over periods of several months in living mice. J. Neurosci. *7*, 1215–1222.

Lowel, S., and Singer, W. (1992). Selection of intrinsic horizontal connections in the visual cortex by correlated neuronal activity. Science *255*, 209–212.

Majewska, A., and Sur, M. (2003). Motility of dendritic spines in visual cortex in vivo: Changes during the critical period and effects of visual deprivation. Proc. Natl. Acad. Sci. USA *100*, 16024–16029.

Maletic-Savatic, M., Malinow, R., and Svoboda, K. (1999). Rapid dendritic morphogenesis in CA1 hippocampal dendrites induced by synaptic activity. Science *283*, 1923–1927.

Malinow, R., and Malenka, R.C. (2002). AMPA receptor trafficking and synaptic plasticity. Annu. Rev. Neurosci. *25*, 103–126.

Maravall, M., Koh, I.Y., Lindquist, W.B., and Svoboda, K. (2004). Experience-dependent changes in basal dendritic branching of layer 2/3 pyramidal neurons during a critical period for developmental plasticity in rat barrel cortex. Cereb. Cortex *14*, 655–664.

Matsuzaki, M., Ellis-Davies, G.C., Nemoto, T., Miyashita, Y., Iino, M., and Kasai, H. (2001). Dendritic spine geometry is critical for AMPA receptor expression in hippocampal CA1 pyramidal neurons. Nat. Neurosci. *4*, 1086–1092.

Matsuzaki, M., Honkura, N., Ellis-Davies, G.C., and Kasai, H. (2004). Structural basis of long-term potentiation in single dendritic spines. Nature *429*, 761–766.

Mizrahi, A., and Katz, L.C. (2003). Dendritic stability in the adult olfactory bulb. Nat. Neurosci. *6*, 1201–1207.

Niell, C.M., Meyer, M.P., and Smith, S.J. (2004). In vivo imaging of synapse formation on a growing dendritic arbor. Nat. Neurosci. *7*, 254–260.

Nimchinsky, E.A., Sabatini, B.L., and Svoboda, K. (2002). Structure and function of dendritic spines. Annu. Rev. Physiol. *64*, 313–353.

Nimchinsky, E.A., Yasuda, R., Oertner, T.G., and Svoboda, K. (2004). The number of glutamate receptors opened by synaptic stimulation in single hippocampal spines. J. Neurosci. *24*, 2054–2064.

Nusser, Z., Lujan, R., Laube, G., Roberts, J.D., Molnar, E., and Somogyi, P. (1998). Cell type and pathway dependence of synaptic AMPA receptor number and variability in the hippocampus. Neuron *21*, 545–559.

Oheim, M., Beaurepaire, E., Chaigneau, E., Mertz, J., and Charpak, S. (2001). Two-photon microscopy in brain tissue: parameters influencing the imaging depth. J. Neurosci. Methods *111*, 29–37.

Peters, A., and Kaiserman-Abramof, I.R. (1970). The small pyramidal neuron of the rat cerebral cortex. The perikaryon, dendrites and spines. Am. J. Anat. *127*, 321–355.

Pologruto, T.A., Sabatini, B.L., and Svoboda, K. (2003). ScanImage: Flexible software for operating laser scanning microscopes. Biomed. Eng. Online *2*, 13.

Portera-Cailliau, C., Pan, D.T., and Yuste, R. (2003). Activity-regulated dynamic behavior of early dendritic protrusions: evidence for different types of dendritic filopodia. J. Neurosci. *23*, 7129–7142.

Racca, C., Stephenson, F.A., Streit, P., Roberts, J.D., and Somogyi, P. (2000). NMDA receptor content of synapses in stratum radiatum of the hippocampal CA1 area. J. Neurosci. *20*, 2512–2522.

Ramon y Cajal, S. (1893). Neue Darstellung vom histologischen Bau des Centralnervensystems. Arch. Anat. Physiol. Anat. Abt. Suppl., 319–428.

Sawtell, N.B., Frenkel, M.Y., Philpot, B.D., Nakazawa, K., Tonegawa, S., and Bear, M.F. (2003). NMDA receptor-dependent ocular dominance plasticity in adult visual cortex. Neuron *38*, 977–985.

Shepherd, G.M., Pologruto, T.A., and Svoboda, K. (2003). Circuit analysis of experience-dependent plasticity in the developing rat barrel cortex. Neuron *38*, 277–289.

Spacek, J. (1985). Three-dimensional analysis of dendritic spines. II. Spine apparatus and other cytoplasmic components. Anat. Embryol. (Berl.) *171*, 235–243.

Stepanyants, A., Hof, P.R., and Chklovskii, D.B. (2002). Geometry and structural plasticity of synaptic connectivity. Neuron *34*, 275–288.

Stern, E.A., Maravall, M., and Svoboda, K. (2001). Rapid development and plasticity of layer 2/3 maps in rat barrel cortex in vivo. Neuron *31*, 305–315.

Svoboda, K., Tank, D.W., and Denk, W. (1996). Direct measurement of coupling between dendritic spines and shafts. Science *272*, 716–719.

Takumi, Y., Ramirez-Leon, V., Laake, P., Rinvik, E., and Ottersen, O.P. (1999). Different modes of expression of AMPA and NMDA receptors in hippocampal synapses. Nat. Neurosci. *2*, 618–624.

Toni, N., Buchs, P.A., Nikonenko, I., Bron, C.R., and Muller, D. (1999). LTP promotes formation of multiple spine synapses between a single axon terminal and a dendrite. Nature *402*, 421–425.

Trachtenberg, J.T., Chen, B.E., Knott, G.W., Feng, G., Sanes, J.R., Welker, E., and Svoboda, K. (2002). Long-term in vivo imaging of experience-dependent synaptic plasticity in adult cortex. Nature *420*, 788–794.

Turner, A.M., and Greenough, W.T. (1985). Differential rearing effects on rat visual cortex synapses. I. Synaptic and neuronal density and synapses per neuron. Brain Res. *329*, 195–203.

Vaughn, J.E., and Peters, A. (1973). A three dimensional study of layer I of the rat parietal cortex. J. Comp. Neurol. *149*, 355–370.

Walsh, M.K., and Lichtman, J.W. (2003). In vivo time-lapse imaging of synaptic takeover associated with naturally occurring synapse elimination. Neuron *37*, 67–73.

Wang, X., Merzenich, M.M., Sameshima, K., and Jenkins, W.M. (1995). Remodelling of hand representation in adult cortex determined by timing of tactile stimulation. Nature *378*, 71–75.

Zhu, J.J. (2000). Maturation of layer 5 neocortical pyramidal neurons: amplifying salient layer 1 and layer 4 inputs by Ca2+ action potentials in adult rat tuft dendrites. J. Physiol. *526*, 571–587.

Ziv, N.E., and Smith, S.J. (1996). Evidence for a role of dendritic filopodia in synaptogenesis and spine formation. Neuron *17*, 91–102.